Langevin modes analysis of myoglobin

Anjum Ansari

Citation: The Journal of Chemical Physics **110**, 1774 (1999); doi: 10.1063/1.477885
View online: http://dx.doi.org/10.1063/1.477885
View Table of Contents: http://scitation.aip.org/content/aip/journal/jcp/110/3?ver=pdfcov
Published by the AIP Publishing

Langevin modes analysis of myoglobin

Anjum Ansari
Department of Physics (M/C 273), University of Illinois at Chicago, Chicago, Illinois 60607-7059

(Received 16 June 1998; accepted 12 October 1998)

Langevin modes describe the behavior of atoms moving on a harmonic potential surface subject to viscous damping described by a classical Langevin equation. We present applications to myoglobin. The Langevin modes are obtained from the gas-phase normal modes using a perturbation expansion. The friction matrix in the Langevin description is assumed diagonal thus ignoring hydrodynamic interactions. The diagonal elements, which are the atomic friction constants on each atom, are weighted according to the surface area accessible to the solvent. Time-dependence of the position and velocity correlation functions are calculated for the Fe atom buried inside the protein for varying values of the external solvent viscosity. Even for negligibly small values of the viscosity, the time correlation functions are overdamped and suggest a substantial damping component from the neighboring protein atoms. The effective friction seen by the Fe atom has contributions from both the solvent friction as well as the internal protein friction. The internal protein friction is estimated to be about 14 ps^{-1} and is comparable to the friction of water. The viscosity dependence of the inverse of the effective friction on the Fe atom is found to agree qualitatively with the viscosity dependence of the experimentally measured rate of conformational changes in myoglobin. © *1999 American Institute of Physics.* [S0021-9606(99)50303-6]

I. INTRODUCTION

In order to accurately characterize the transition state along a reaction pathway, it is important to separate the damping effects of the solvent on the rate processes and to study the temperature dependence of the activated step. The validity of using the transition state theory of Eyring and co-workers to describe rate processes in proteins has been investigated by a number of researchers.[1–9] The transition state theory does not take into account any damping effects of the external medium and results in incorrect estimation of the barrier heights. Moreover, proteins are a medium in themselves, and there are damping effects owing to the internal degrees of freedom in the protein. An experimental and theoretical understanding of these damping effects is necessary to correctly interpret activated rate processes in proteins.

The theoretical explanation for the damping effects of the solvent on the rate of chemical reactions is due to Kramers[10] who idealized a chemical reaction as the Brownian motion of a particle in the presence of a potential energy barrier. Kramers' behavior has been observed in the photochemical isomerization of dye molecules in solution[11–13] and, more recently, in some experimental[14] and theoretical[15] studies of protein folding. In large macromolecules, like the protein, the friction can have two contributions: the solvent friction due to collisions with the solvent molecules as well as internal or ''protein'' friction due to the internal degrees of freedom of the protein that are not explicitly included in the reaction coordinate. Is the Kramers' picture applicable in a complicated $3N$-dimensional conformational space of proteins? The results of Ansari *et al.*,[7,8] in which the viscosity dependence of a pure conformational change in myoglobin (Mb) was investigated in detail, suggest that Kramers' theory does very well in the high viscosity regime but shows deviations at low viscosities. This deviation was explained by assuming that the protein friction and the solvent friction are additive along the reaction coordinate and that, at low solvent viscosities, the protein friction dominates. The damping effects due to internal friction have been observed in the dynamical behavior of side-chains in molecular dynamics simulations of bovine pancreatic trypsin inhibitor (BPTI).[16] Loncharich *et al.*[17] have done Langevin dynamics simulations on a small peptide (N-Acetylalanyl-N'-Methylamide) and measured the isomerization rate as a function of the externally applied friction. In the high friction limit they reproduce Kramers' behavior for the rate of isomerization, but show deviations at low values of the friction where the rate saturates. The simulations of Loncharich *et al.*[17] suggest that the internal friction of a small peptide is of the order of 10–100 times smaller than that of water. In a large protein with many more degrees of freedom the internal friction is expected to be much larger. In this paper we analyze the dynamical behavior of internal atoms in myoglobin placed in a solvent bath and describe the system using the classical Langevin equations. The solution of the Langevin equations reduces to a set of coupled ''Langevin modes'' when the interaction potential is assumed to be harmonic.[18] The dynamical behavior of the atoms is expressed as correlation functions in terms of these Langevin modes using the formulation developed by Lamm and Szabo.[18] The calculation is done for varying values of the external friction in order to estimate the contribution of internal friction and to test the assumption of Ansari *et al.*[7,8] that the contributions from internal and external friction are simply additive. Although anharmonic effects are clearly important in proteins, it is nevertheless a useful exercise to examine the simplest description that includes the damping effects of the solvent.

II. LANGEVIN MODES DESCRIPTION

A. Theory

The relevant theoretical results of the ''Langevin modes'' description of Lamm and Szabo[18] and its application to Mb is described here. For a macromolecule consisting of N atoms whose positions are specified by Cartesian coordinates $q_{i\alpha}$, $i=1,...,N$ and $\alpha=1,...,3$ for the three degrees of freedom, and which is immersed in a bath that exerts forces on the individual atoms, the dynamics can be described by a set of coupled Langevin equations,

$$m_i\ddot{q}_{i\alpha}+\sum_{(j\beta)=1}^{3N}\zeta_{(i\alpha)(j\beta)}\dot{q}_{j\beta}+\sum_{(j\beta)=1}^{3N}\left(\frac{\partial^2 V}{\partial q_{i\alpha}\partial q_{j\beta}}\right)_{q^0}\Delta q_{j\beta} =R_{i\alpha}(t), \quad (i\alpha)=1,...,3N, \tag{1}$$

where m_i denotes the mass of the ith atom, $\Delta q_{i\alpha}$ the deviations from the equilibrium positions, $\boldsymbol{\zeta}$ the friction matrix, V the interaction potential, and $R_{i\alpha}$ the random forces from fluctuations in the solvent. In the absence of any external friction ($\boldsymbol{\zeta}=0$), Eq. (1) reduces to Newton's equations of motion and the dynamics of the system is described in terms of $3N$ normal modes which are independent oscillators described by the eigenvectors $\mathbf{U}$ of the mass-weighted second derivative matrix $\mathbf{F}$,

$$F_{(i\alpha)(j\beta)}=\frac{1}{\sqrt{m_i m_j}}\left(\frac{\partial^2 V}{\partial q_{i\alpha}\partial q_{j\beta}}\right) \tag{2}$$

and with oscillation frequencies ω_n for the nth normal mode given by the square-root of the eigenvalues of the matrix $\mathbf{F}$. In this paper we limit our discussion to the zeroeth order solution of Eq. (1) in which an approximate solution to the full Langevin problem is obtained as a perturbation of the normal mode analysis.[18] The normal mode analysis requires diagonalization of a symmetric $3N\times 3N$ matrix whereas the complete solution requires diagonalization of a nonsymmetric $6N\times 6N$ matrix and is considerably more computer-intensive. It is worth noting that Kottalam and Case[19] compared the results from a perturbation analysis with the complete Langevin modes description for the protein crambin and a short DNA oligomer and found very good agreement between relaxation times describing the solvent damping of each damped mode. The dynamics in the perturbation analysis is described in terms of $3N$ independent harmonic oscillators that are damped. The damping constant or collision frequency corresponding to the nth oscillator, denoted by Γ_n, is given by the diagonal elements of the matrix $\mathbf{U}^T\boldsymbol{\gamma}\mathbf{U}$, where $\boldsymbol{\gamma}$ is the mass-weighted friction matrix,

$$\gamma_{(i\alpha)(j\beta)}=\frac{1}{\sqrt{m_i m_j}}\,\zeta_{(i\alpha)(j\beta)}. \tag{3}$$

The zeroeth order eigenvalues of the Langevin mode problem, denoted by λ_0, are given by

$$\lambda_0=\frac{1}{2}\begin{pmatrix}-\boldsymbol{\Gamma}+\boldsymbol{\Delta} & 0\\ 0 & -\boldsymbol{\Gamma}-\boldsymbol{\Delta}\end{pmatrix}, \tag{4}$$

where $\boldsymbol{\Gamma}$ is a diagonal matrix with elements Γ_n and $\boldsymbol{\Delta}$ is a diagonal matrix with elements $\Delta_n=\sqrt{\gamma_n^2-4\omega_n^2}$. The Langevin eigenvalues are either real and negative (for overdamped modes) or occur in complex conjugate pairs (for underdamped modes).

A useful description of the dynamical behavior of individual atoms in the protein is provided by the time-evolution of the position and velocity correlation functions. The set of equations that describe the position and velocity correlations functions in terms of Langevin modes are

$$\langle\Delta q_{i\alpha}(t)\cdot\Delta q_{i\alpha}(0)\rangle=\frac{k_BT}{m_i}\sum_{n=1}^{3N-6}\frac{U_{(i\alpha)n}^2}{\omega_n^2}\,\theta_n(t),$$
$$\langle\dot{q}_{i\alpha}(t)\cdot\dot{q}_{i\alpha}(0)\rangle=\frac{k_BT}{m_i}\sum_{n=1}^{3N-6}U_{(i\alpha)n}^2\,\theta_n'(t), \tag{5}$$

where the normal modes corresponding to pure translation and pure rotation are not included in the sum. $\theta_n(t)$ and $\theta_n'(t)$ describe the time-dependence of the position and velocities, respectively, of the nth damped oscillator,

$$\theta_n(t)=\exp(-\Gamma_n t/2)\left[\cosh(\Delta_n t/2)+\frac{\Gamma_n}{\Delta_n}\sinh(\Delta_n t/2)\right],$$
$$\theta_n'(t)=\exp(-\Gamma_n t/2)\left[\cosh(\Delta_n t/2)-\frac{\Gamma_n}{\Delta_n}\sinh(\Delta_n t/2)\right]. \tag{6}$$

B. Model: Assignment of friction matrix

The first step in the Langevin mode description is to define the $3N\times 3N$ friction matrix $\boldsymbol{\zeta}$, the diagonal elements of which are the atomic friction constants on each atom for each degree of freedom, and the off-diagonal elements describe hydrodynamic interactions between the atoms. The empirical formula of Pastor and Karplus[20] was used to assign the atomic friction constants as

$$\zeta_{(i\alpha)(i\alpha)}=4\pi\eta_s a_i^{\mathrm{eff}} \ \text{ for all } \ \alpha, \tag{7}$$

where η_s is the solvent viscosity and a_i^{eff} is the effective hydrodynamic radius for the ith atom such that $4\pi(a_i^{\mathrm{eff}})^2$ is equal to the surface area accessible to the solvent. This assignment of the atomic friction constants was shown to provide a good agreement with the calculated and experimen-

tally observed translational and rotational diffusion constants for macromolecules.[21] The exposed surface area for each atom was calculated with the CHARMM program[22] using the algorithm of Lee and Richards[23] and with a probe radius of 1.4 Å. The assignment of the off-diagonal terms describing hydrodynamic interactions between different protein atoms is nontrivial since, for many pairs of atoms, the intervening space is filled with other protein atoms rather than with solvent. Hydrodynamic interactions have been ignored in the simplest description. The damping constant for the nth Langevin mode is then given by

$$\Gamma_n = \sum_{(i\alpha)=1}^{3N-6} U_{(i\alpha)n} \frac{\zeta_{(i\alpha)(i\alpha)}}{m_i} U_{(i\alpha)n}. \tag{8}$$

III. RESULTS

A. Normal mode calculation

The coordinate set for Mb used for the normal mode calculations is the CO-complex from Kuriyan *et al.*[24] and all calculations were done on the HP-755 using the CHARMM program. The standard force field for CHARMM19 was used with nonpolar hydrogen atoms represented by corresponding extended-type carbon atoms, thus reducing the total number of atoms from 2536 to 1530. Shift cutoff conditions with a cutoff distance of 12 Å were used for both the Lennard-Jones and the Coulomb interactions.[25] A relative dielectric coefficient proportional to the distance was used. Prior to the normal mode calculation the total energy of the protein was minimized to ensure that the first derivatives of the interaction potential are close to zero. Upon minimization, the rms value for the elements of the gradient vector was 10^{-5} kcal/mol/Å. The mass-weighted structural drift from the original x-ray coordinates was 1.59 Å and 1.25 Å, respectively, for all protein atoms and backbone atoms.

Since we are interested in the global motions of the protein, we include only the low frequency modes in our calculations. The high frequency modes corresponding to the internal vibrational degrees of freedom of the individual atoms are expected to be independent of the external friction and are not included in the present analysis. All the results presented here use only the first 1000 normal modes for further calculations in order to reduce the computational time and memory for data storage. High frequency modes with oscillation frequencies larger than about 40 ps^{-1} have been neglected. The first few nonzero eigenvalues obtained from our normal mode analysis are 0.358, 0.43, 0.662, 1.124, 1.222, 1.406,..., ps^{-1}. The first value agrees very well with the corresponding eigenvalue ($=12.74$ cm^{-1}; 0.382 ps^{-1}) reported by Melchers *et al.*[26] in their normal mode analysis of MbCO.

The damping constant Γ_n for each mode was calculated as a function of the external solvent viscosity using Eqs. (7) and (8). Figure 1(a) shows the damping constant as a function of the oscillation frequency for each normal mode when the solvent viscosity is 1 cP. The damping constant is about 10 ps^{-1} for the lowest frequency mode and decreases to about 7 ps^{-1} for the highest frequency reported in this study. Figures 1(b) and 1(c) show the real and imaginary parts of the Langevin eigenvalues calculated using Eq. (4). At a solvent viscosity of 1 cP the modes with frequencies below ~5 ps^{-1} are overdamped as indicated by the purely real Langevin eigenvalues. For each overdamped mode ($\Gamma_n > 2\omega_n$) there are two real negative eigenvalues. For the underdamped modes the imaginary part of the eigenvalue corresponds to the oscillation frequency of the mode.

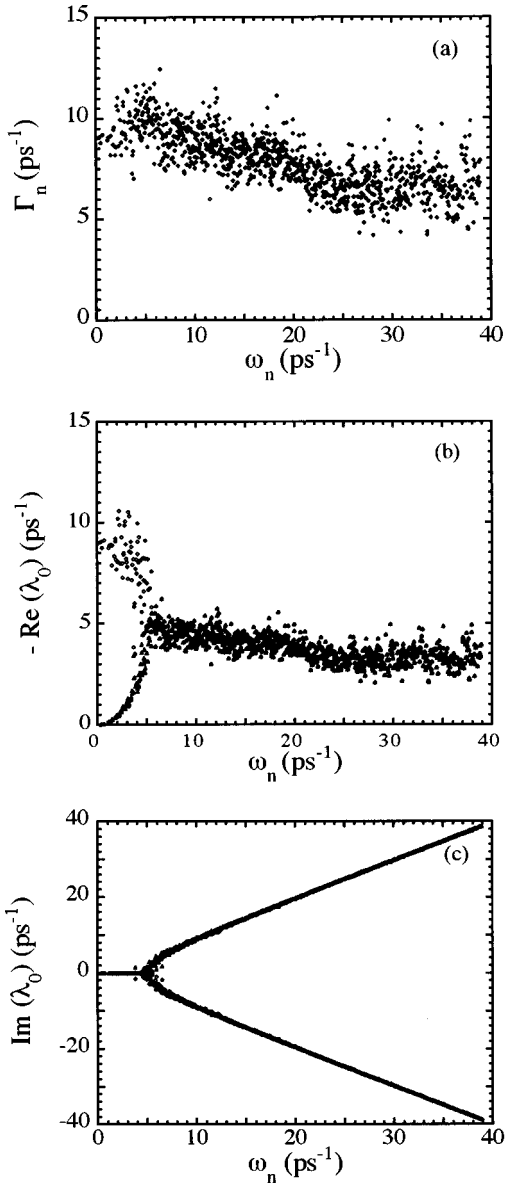

FIG. 1. Results of the Langevin modes analysis for $\eta_s = 1$ cP. (a) The damping constant Γ_n for the nth Langevin mode, calculated using Eqs. (7) and (8), is plotted vs the normal mode frequency ω_n. (b) and (c) The real and the imaginary parts of the Langevin eigenvalues λ_0, calculated using Eq. (4), are plotted vs the normal mode frequency ω_n. The time constant for the solvent damping of each mode is given by $-1/\mathrm{Re}(\lambda_0)$.

B. Correlation functions

The correlation functions are a measure of the decay of a fluctuation in the displacement or velocity of an atom and are useful in describing the dynamical character of the fluctuation. For instance, for an undamped oscillator the correlation function is oscillatory whereas for an overdamped oscillator the correlation function decays exponentially. The displace-

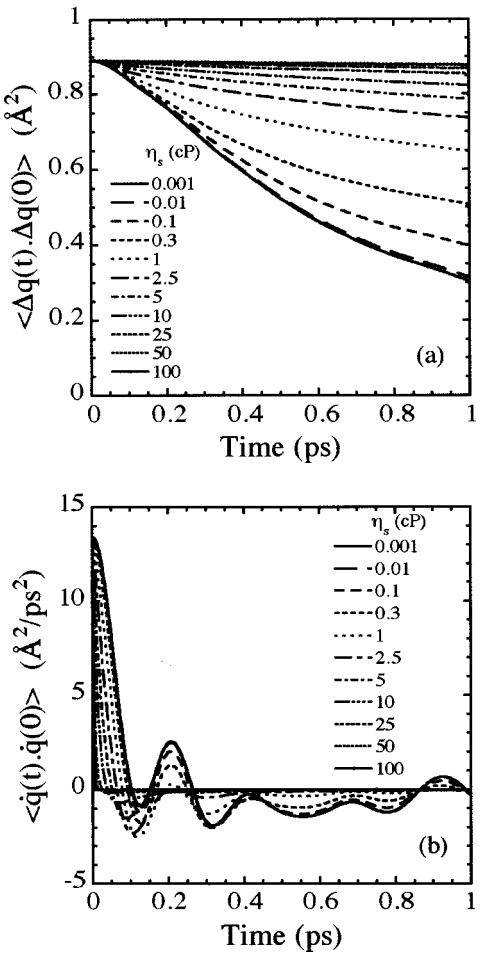

FIG. 2. Position and velocity correlation functions for the Fe atom. (a) The position correlation function, summed over the three degrees of freedom [Eq. (9)], is plotted vs time for various values of the external (solvent) viscosity η_s. The slowest decaying function corresponds to the highest value of η_s. (b) The velocity correlation function, summed over the three degrees of freedom, is plotted vs time for the same set of values of η_s. The fastest decaying function corresponds to the highest value of η_s.

ment and velocity of an individual atom is a superposition of all the Langevin modes. Since we are not using all the normal modes in our calculations, the correlation functions have to be appropriately normalized so as to yield the correct initial values. Furthermore, the correlation functions along the three coordinates are, of course, dependent on the orientation of the molecule relative to the axes defined in the coordinate file. The sum of the three correlation functions is, however, independent of the orientation. The correlation functions for each atom i were therefore calculated as follows:

$$\langle \Delta q_i(t)\cdot\Delta q_i(0)\rangle = \sum_{\alpha=1}^{3} \frac{k_B T}{m_i} \frac{\Sigma_{n=1}^{994} \frac{U_{(i\alpha)n}^2}{\omega_n^2}\,\theta_n(t)}{\Sigma_{n=1}^{994} U_{(i\alpha)n}^2},$$
$$\langle \dot{q}_i(t)\cdot\dot{q}_i(0)\rangle = \sum_{\alpha=1}^{3} \frac{k_B T}{m_i} \frac{\Sigma_{n=1}^{994} U_{(i\alpha)n}^2\,\theta_n'(t)}{\Sigma_{n=1}^{994} U_{(i\alpha)n}^2}, \tag{9}$$

where the sum over α refers to the sum over the three coordinates for each atom. Figure 2 shows the displacement and the velocity correlation functions for the Fe atom as a function of time for various values of the solvent viscosity η_s and shows an overdamped behavior. The residual oscillations observed in the velocity correlation functions may be a consequence of not including all the normal modes in the calculation.

C. Calculation of the internal (protein) friction

It is clear from the results of Fig. 2 that the dynamical behavior of the Fe atom is damped by internal motions of the protein when the external friction from the solvent viscosity approaches zero. We have made an estimate of this internal protein friction using two approaches that are described below.

The position and velocity correlation functions of a three-dimensional damped harmonic oscillator with an effective damping constant (γ_{eff}) and an effective frequency (ω_{eff}) are given by

$$\langle \Delta q(t)\cdot\Delta q(0)\rangle = \frac{3k_B T}{m\omega_{\text{eff}}^2} \exp\left(-\frac{\gamma_{\text{eff}} t}{2}\right) \times\left[\cosh\left(\frac{\Delta_{\text{eff}} t}{2}\right) + \frac{\gamma_{\text{eff}}}{\Delta_{\text{eff}}}\sinh\left(\frac{\Delta_{\text{eff}} t}{2}\right)\right],$$
$$\langle \dot{q}(t)\cdot\dot{q}(0)\rangle = \frac{3k_B T}{m} \exp\left(-\frac{\gamma_{\text{eff}} t}{2}\right) \times\left[\cosh\left(\frac{\Delta_{\text{eff}} t}{2}\right) - \frac{\gamma_{\text{eff}}}{\Delta_{\text{eff}}}\sinh\left(\frac{\Delta_{\text{eff}} t}{2}\right)\right], \tag{10}$$

where $\Delta_{\text{eff}} = \sqrt{\gamma_{\text{eff}}^2 - 4\omega_{\text{eff}}^2}$. The decay of the position and velocity correlation functions of individual atoms in proteins are due to the superposition of all the Langevin modes. We may, however, estimate the value of the effective friction on the Fe atom by fitting the initial decay to the function for a damped 3D harmonic oscillator [Eq. (10)]. The effective frequency ω_{eff}, which is an equilibrium quantity and is independent of the friction, was calculated from the average value of the displacement squared (summed over the three independent coordinates) as

$$\omega_{\text{eff}} = \sqrt{\frac{3k_B T}{m_i\langle \Delta q_i(t)^2\rangle}}. \tag{11}$$

The factor 3 in Eqs. (10) and (11) comes from the sum over the three coordinates for each atom. For the Fe atom $\langle \Delta q_i(t)^2\rangle = 0.89\ \text{Å}^2$ (at $T = 300$ K) and $m = 55.85$ amu, yielding a value of $\omega_{\text{eff}} = 3.88\ \text{ps}^{-1}$. The position correlation functions were fit to Eq. (10) with γ_{eff} as a fitting parameter for each value of the external solvent viscosity. The fit is reasonably good out to about 0.1 ps [Fig. 3(a)]. The velocity correlation functions are not approximated very well by the expression for a damped oscillator except at high solvent viscosities [Fig. 3(b)] and were not included in the fit. The effective damping constant on the Fe atom as a function of the external solvent viscosity is plotted in Fig. 5(b).

The second approach used the area under the velocity correlation function as an estimate of the effective friction. In the limit of Brownian or overdamped motion, the decay of the velocity correlation function provides an approximate measure of the effective diffusion constant D_{eff},

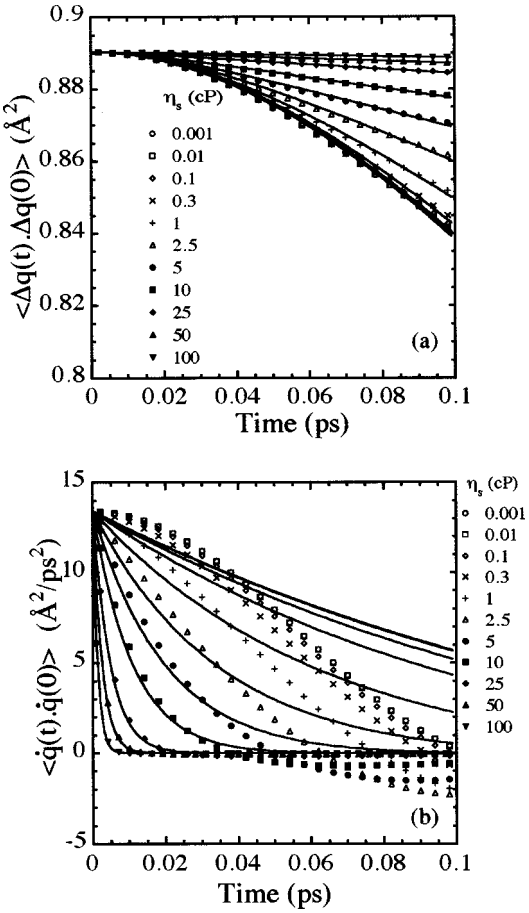

FIG. 3. Results of a fit to a three-dimensional damped harmonic oscillator model. (a) The data of Fig. 2(a) (shown in symbols) is fit to the equation for a damped oscillator [Eq. (10)] with γ_{eff} as the fitting parameter for each curve. The fitted curves are drawn as solid lines. The effective frequency ω_{eff} is obtained from Eq. (11) and has a value of 3.88 ps^{-1}. The data is fit up to 0.1 ps. Including more data points makes the fit successively worse. The values of γ_{eff} obtained from the fit are plotted in Fig. 5(b). (b) The velocity correlation functions for a damped oscillator, calculated using Eq. (10) for each value of γ_{eff}, are plotted as solid lines. The data of Fig. 2(b) (shown in symbols) is also plotted for comparison. The damped harmonic oscillator model approximates the velocity correlation functions only for the high damping conditions.

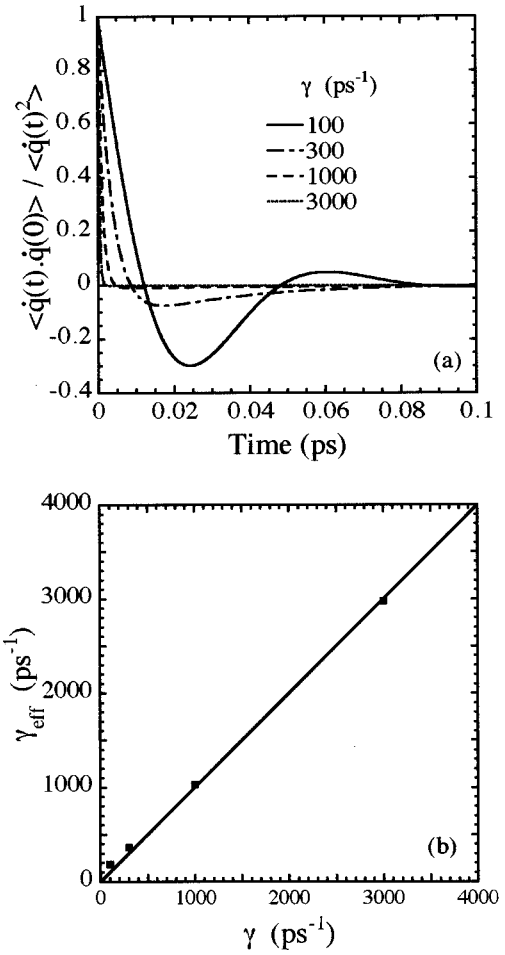

FIG. 4. Damped harmonic oscillator. (a) Velocity correlation functions, as defined in Eq. (10) and normalized for the amplitude, are plotted for $\omega = 100\ \text{ps}^{-1}$ and for values of the damping constant $\gamma = 100$, 300, 1000, and 3000 ps^{-1}, respectively. (b) The effective values of the damping constant γ_{eff} for the velocity correlation functions plotted in Fig. 4(a), estimated using the relation $\gamma_{\text{eff}} = \langle \dot{q}(t)^2 \rangle / \int_0^{\Delta t} \langle \dot{q}(s) \cdot \dot{q}(0) \rangle ds$, are plotted against the actual values of the damping constant. The solid line is plotted at 45°.

$$D_{\text{eff}} \cong \frac{1}{3} \int_0^{\Delta t} \langle \dot{q}(s) \cdot \dot{q}(0) \rangle ds, \tag{12}$$

where the integration extends over times that are comparable to the time over which the correlation function tends to zero.[27] Using the relation

$$\gamma_{\text{eff}} = \frac{k_B T}{m D_{\text{eff}}} \tag{13}$$

we can obtain a value of γ_{eff} that does not require modeling the dynamics as that of a damped oscillator. The validity of this approach is demonstrated by simulating the velocity correlation functions for a damped harmonic oscillator for various values of the friction, and using Eqs. (12) and (13) to estimate the value of the friction. The value of Δt in Eq. (12) was taken to be the time at which the velocity correlation function crosses zero for the first time. The results of the calculation are plotted in Fig. 4 and show that for highly damped systems the above approach provides a reasonable estimate of the friction. For the system under study γ_{eff} was obtained from the data in Fig. 2(b) and Eqs. (12) and (13) and these results are also plotted in Fig. 5(b).

D. Comparison with experiment

The rate of the conformational change in Mb for varying solvent viscosities was investigated in detail by Ansari *et al.*[7,8] They showed that the rate was independent of the viscosity at low solvent viscosities ($\eta_s < 4$ cP) and inversely proportional to the viscosity at high viscosities ($\eta_s > 10$ cP). This result was explained in the framework of Kramers' theory[10,28] by assuming that the friction term along the reaction coordinate has two contributions; one from the solvent friction (which retards the motions of atoms on the surface of the protein) and the other from the protein friction (which slows the motions of protein atoms relative to one another). If the two contributions are additive, the Kramers equation for the rate constant in the high friction limit becomes

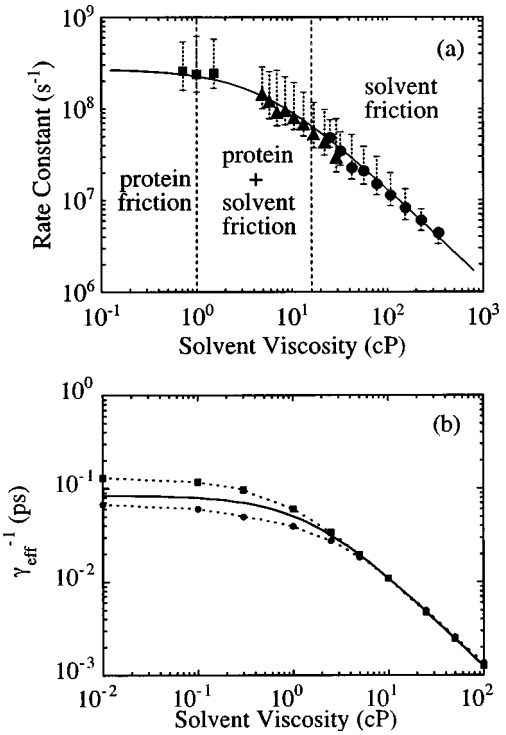

FIG. 5. Comparison of the rate of the conformational change in Mb and the effective friction on the Fe atom as a function of the external solvent viscosity. (a) Rate constant for Mb conformational change is plotted as a function of solvent viscosity. The data is reproduced from Ansari *et al.* (Ref. 7). (b) The inverse of the effective friction on the Fe atom ($1/\gamma_{\text{eff}}$) is plotted as a function of the external solvent viscosity. (■) The values are obtained from the fit to the position correlation function shown in Fig. 2(a); (●) The values are obtained from the data in Fig. 2(b) and Eqs. (12) and (13), where Δt for each curve is taken to be the time at which the velocity correlation function approaches zero for the first time. The solid line is a fit to the data using Eq. (16).

$$k=\frac{B}{\alpha\zeta_p+(1-\alpha)\zeta_s}\exp(-E_0/RT), \tag{14}$$

where R is the gas constant, T is the temperature, E_0 is the average height of the potential energy barrier separating the protein conformations, B is a viscosity- and temperature-independent parameter that depends on the shape of the potential surface, ζ_p is the friction coefficient for motion in the protein, and ζ_s is the friction coefficient for motion in the solvent which, according to Stokes' law, is proportional to its viscosity. To apply Eq. (14) to the experimental data, the pre-exponential factor was written in terms of the known solvent viscosity, and adjustable parameters C and σ,

$$k=\frac{C}{\sigma+\eta_s}\exp(-E_0/RT), \tag{15}$$

where σ has units of viscosity. The fit to the experimentally observed rates using Eq. (15) is shown in Fig. 5(a) with a value of $\sigma=4$ cP.

In order to compare the results of the Langevin modes analysis with the experimental results obtained by Ansari *et al.*[7,8] the inverse of the effective damping constant, $1/\gamma_{\text{eff}}$, is plotted vs the solvent viscosity in Fig. 5(b). The shape of the two curves are in remarkable agreement with a turnover observed at viscosities corresponding to that of water. The data in Fig. 5(b) are fit to the functional form,

$$\gamma_{\text{eff}}=\alpha\gamma_p+(1-\alpha)\gamma_s, \tag{16}$$

and yield a value of $\gamma_p=13.6\ \text{ps}^{-1}$ and $\alpha=0.87$. The values of γ_s (in ps^{-1}) are taken to be $\eta_s\times 60$ where η_s is in cP. These results suggest that the effective internal friction of the protein is comparable to the friction of water ($\gamma_s \approx 60\ \text{ps}^{-1}$).

IV. CONCLUSIONS

Langevin modes analysis provides a simple way of looking at the dynamics of macromolecules in the presence of a solvent. The Langevin modes presented here have been obtained from the normal modes using a perturbation expansion which is the zeroth order description that includes frictional effects. The analysis presented here is very simplified and does not include hydrodynamic interactions. Furthermore, since we are interested only in the global motions of the protein that are involved in large-scale conformational changes, the high frequency modes have been neglected. Despite these approximations the results provide some useful insight into the dynamics of proteins which are not so easily accessible with Langevin dynamics simulations. In particular, time correlation functions require long simulations for any reasonable signal averaging.[29] We have used this simplified description in order to make comparisons with experimental results on the dynamics of Mb.

Measurements of the dynamics of conformational changes in Mb had showed that the rate constant for global conformational changes was inversely proportional to the solvent viscosity at high viscosities but was independent of the viscosity at low viscosities. This result was explained by assuming that the friction along the reaction coordinate has contributions from both the protein and the solvent friction. In this paper we show that the low frequency dynamics of the Fe atom buried inside the protein is also influenced by a combination of the external solvent friction and the protein friction; in fact the assumption made in Eq. (14) describing the functional form of the effective friction along the reaction coordinate is borne out by the effective friction on the Fe atom. The reason for choosing the Fe atom to display the results of the Langevin modes analysis are twofold; one is that the Fe atom is completely buried inside the protein and therefore should see the protein friction most effectively, and two, because the displacement of the Fe atom is strongly coupled to the global conformational change that occurs in Mb upon deoxygenation.[24]

There is some evidence from molecular dynamics analysis of a zinc-finger peptide[30] that the Langevin modes description overdamps the decay of correlation functions describing the internal reorientational dynamics of nuclear spin pairs compared to the decays obtained using a full molecular dynamics simulations with explicit solvent. The reorientational dynamics of individual nuclear spins are, of course, primarily dominated by high frequency local motions. Go and co-workers have investigated the effects of solvent on the collective motions of melittin[31] and BPTI.[32] They describe the dynamics in terms of principal modes obtained

from molecular dynamics trajectories in vacuum and in water. They have also carried out a modified Langevin modes description in which the Hessian matrix **F** [Eq. (2)] as well as the friction coefficient matrix $\boldsymbol{\gamma}$ [Eq. (3)] are calculated from a molecular dynamics trajectory with explicit solvent.[31] Their Langevin modes analysis reproduces the results of the simulations in water reasonably well suggesting that this type of analysis may work well for the dynamical aspects that are dominated by the low frequency modes. One major advantage of using the principal modes and the modified Langevin modes is that the effects of solvent-induced changes[33] as well as the anharmonicities in the potential surface are included in the analysis and would represent a more realistic picture of the dynamics. Fine-tuning the calculations presented in this paper by including these ''static'' effects of the solvent, anharmonicities in the potential function, and hydrodynamics interactions would shift somewhat the turning point on the $1/\gamma_{\mathrm{eff}}$ vs η_s curve shown in Fig. 5(b).

It is, perhaps, surprising that the viscosity dependence obtained from these simulations, which look at the dynamics of the Fe atom at the bottom of the harmonic well, are in agreement with the viscosity dependence of the experimentally measured rates which monitor barrier crossing. The fact that the simulations agree qualitatively with the experimental results suggests that by discarding the high frequency modes we are in fact exploring the conformational coordinate that is relevant to the global conformational changes in the protein and that the friction at the bottom of the well is similar to the friction at the top of the barrier.

In conclusion, the results reported in this paper support the assumption that dynamics of proteins are influenced by internal (protein) as well as external (solvent) damping and that, under aqueous conditions, the contributions from internal damping are comparable to that of the solvent. There are many questions remaining: (1) Are these results unique to Mb or a general feature of conformational changes in proteins? (2) How does the protein friction change with the kind of conformational change, i.e., tertiary (which may involve large sections of the protein sliding past one another) and quaternary (which may involve rearrangement of subunits)? (3) How does the protein friction change with temperature? A number of these issues need to be addressed experimentally since modeling realistic conformational changes in proteins is still a computationally daunting task. However, Langevin modes analysis together with Langevin dynamics simulations[19,30,31,34] are useful tools that complement the experiments for a more thorough understanding of the dynamics of proteins in a solvent bath.

ACKNOWLEDGMENTS

I have benefitted from many discussions with Attila Szabo in the preparation of this manuscript. Acknowledgements are due to Peter J. Steinbach and Bernard R. Brooks for providing the minimum energy coordinates of Mb and for help with CHARMM. The normal mode calculations were done at the Laboratory of Chemical Physics at National Institutes of Health, and I am grateful to Eric R. Henry for help with the HP-755.

[1] B. Gavish and M. M. Werber, Biochemistry **18**, 1269 (1979).
[2] D. Beece, L. Eisenstein, H. Frauenfelder, D. Good, M. C. Marden, L. Reinisch, A. H. Reynolds, L. B. Sorenson, and K. T. Yue, Biochemistry **19**, 5147 (1980).
[3] B. Gavish, Phys. Rev. Lett. **44**, 1160 (1980).
[4] N. Agmon and J. J. Hopfield, J. Chem. Phys. **79**, 2042 (1983).
[5] D. Lavalette and C. Tetreau, Eur. J. Biochem. **177**, 97 (1988).
[6] A. P. Demchenko, O. I. Rusyn, and E. A. Saburova, Biochim. Biophys. Acta **998**, 196 (1989).
[7] A. Ansari, C. M. Jones, E. R. Henry, J. Hofrichter, and W. A. Eaton, Science **256**, 1796 (1992).
[8] A. Ansari, C. M. Jones, E. R. Henry, J. Hofrichter, and W. A. Eaton, Biochemistry **33**, 5128 (1994).
[9] M. Lim, T. A. Jackson, and P. A. Anfinrud, in *Proceedings of the 4th International Conference on Laser Applications in Life Sciences* (SPIE, The International Society for Optical Engineering, Berlin, 1993), Vol. 1921, p. 221.
[10] H. A. Kramers, Physica (Utrecht) **7**, 284 (1940).
[11] K. M. Keery and G. Fleming, Chem. Phys. Lett. **93**, 322 (1982).
[12] G. Rothenberger, D. K. Negus, and R. M. Hochstrasser, J. Chem. Phys. **79**, 5360 (1983).
[13] M. Lee, G. R. Holtom, and R. M. Hochstrasser, Chem. Phys. Lett. **118**, 359 (1985).
[14] C. D. Waldburger, T. Jonsson, and R. T. Sauer, Proc. Natl. Acad. Sci. USA **93**, 2629 (1996).
[15] D. K. Klimov and D. Thirumalai, Phys. Rev. Lett. **79**, 317 (1997).
[16] J. A. McCammon, P. G. Wolynes, and M. Karplus, Biochemistry **18**, 927 (1979).
[17] R. J. Loncharich, B. R. Brooks, and R. W. Pastor, Biopolymers **32**, 523 (1992).
[18] G. Lamm and A. Szabo, J. Chem. Phys. **85**, 7334 (1986).
[19] J. Kottalam and D. A. Case, Biopolymers **29**, 1409 (1990).
[20] R. W. Pastor and M. Karplus, J. Phys. Chem. **92**, 2636 (1988).
[21] R. M. Venable and R. W. Pastor, Biopolymers **27**, 1001 (1988).
[22] B. R. Brooks, R. E. Bruccoleri, B. D. Olafson, D. J. States, S. Swaminathan, and M. Karplus, J. Comput. Chem. **4**, 187 (1983).
[23] B. Lee and F. M. Richards, J. Mol. Biol. **55**, 379 (1971).
[24] J. Kuriyan, S. Wilz, M. Karplus, and G. Petsko, J. Mol. Biol. **192**, 133 (1986).
[25] P. J. Steinbach and B. R. Brooks, J. Comput. Chem. **15**, 667 (1994).
[26] B. Melchers, E. W. Knapp, F. Parak, L. Cordone, A. Cupane, and M. Leone, Biophys. J. **70**, 2092 (1996).
[27] R. Zwanzig, Annu. Rev. Phys. Chem. **16**, 67 (1965).
[28] P. Hänggi, P. Talkner, and M. Borkovec, Rev. Mod. Phys. **62**, 251 (1990).
[29] R. W. Pastor, in *Proteins: Structure, Dynamics and Design*, edited by V. Renugopalakrishnan, P. R. Carey, I. C. P. Smith, S. G. Huang, and A. C. Storer (ESCOM Science, Leiden, 1991), p. 229.
[30] A. G. Palmer III and D. A. Case, J. Am. Chem. Soc. **114**, 9059 (1992).
[31] A. Kitao, F. Hirata, and N. Go, Chem. Phys. **158**, 447 (1991).
[32] S. Hayward, A. Kitao, F. Hirata, and N. Go, J. Mol. Biol. **234**, 1207 (1993).
[33] B. M. Pettitt and M. Karplus, Chem. Phys. Lett. **121**, 194 (1985).
[34] R. W. Pastor, in *The Molecular Dynamics of Liquid Crystals*, edited by G. R. Luckhurst and C. A. Veracini (Kluwer Academic, The Netherlands, 1994).